Electronic Supplementary Information

Anticancer Luminescent Gold Quantum Clusters for *In Situ* Cancer-Selective Marking-Imaging-Targeting

Jeong-Hwan Kim,[1] Haruki Eguchi,[2] and Yoshihiro Ishikawa[1]*

[1]Cardiovascular Research Institute, Yokohama City University, Graduate School of Medicine, Yokohama, 236-0004, Japan.

[2]Advanced Applied Science Department, Research Laboratory, IHI Corporation, Yokohama, 235-8501, Japan.

Email: jeongkim@yokohama-cu.ac.jp

This material includes **Fig. S1-S13**.

[Insert Running title of <72 characters]

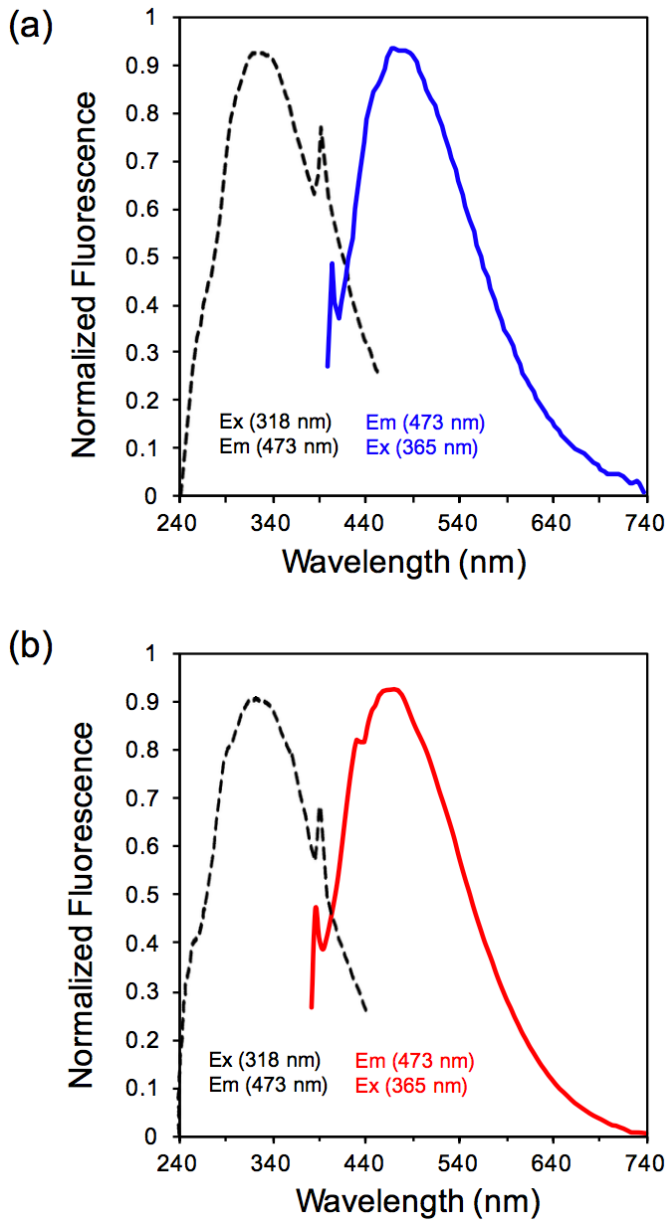

Fig. S1 Normalized fluorescence spectra of (a) Au(en)QC and (b) Tf-Au(en)QC samples, showing identical excitation and emission peaks.

1

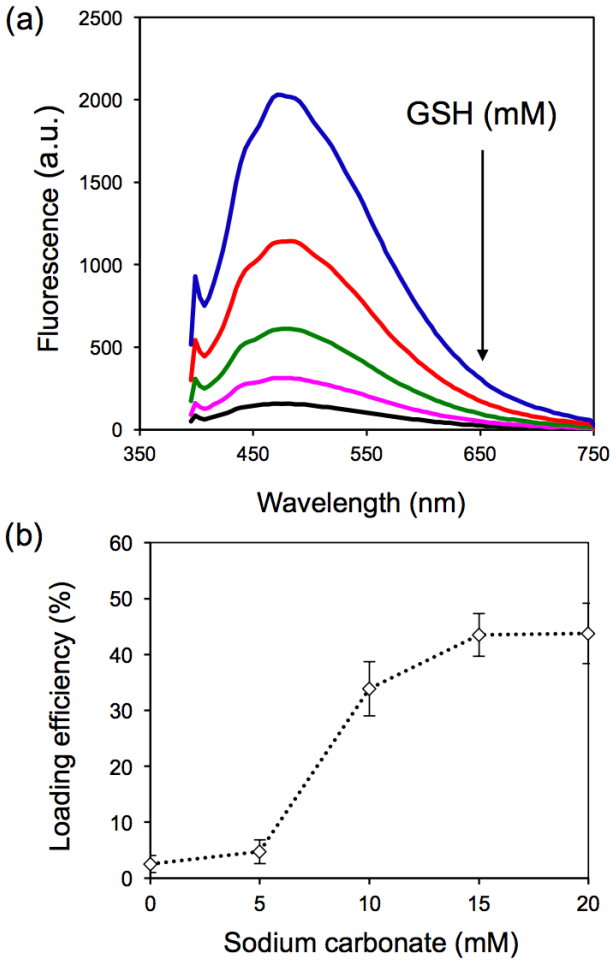

2

3 **Fig. S2** (a) Fluorescence spectra of Au(en)QC samples as a function of GSH

4 concentration, 0, 5, 10, 15, 20 mM (top to bottom). (b) Sodium carbonate-dependent

5 loading efficiency of Au(en)QCs in Tf-Au(en)QC complex.

6

7

8

9

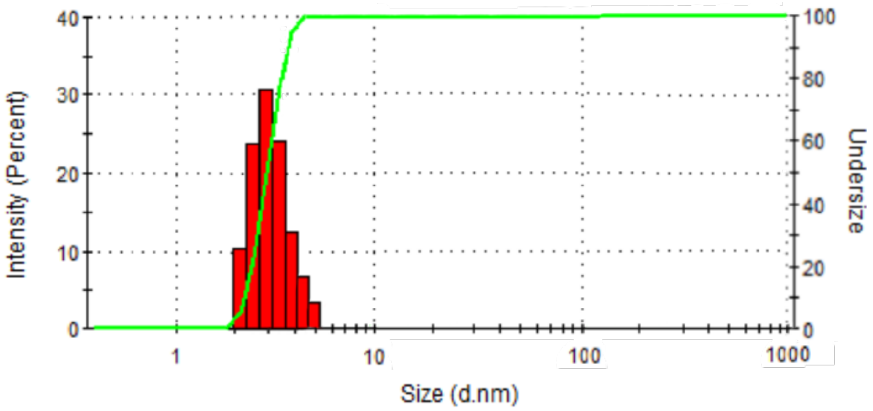

Fig. S3 DLS size distribution of Bt-AuNPs in DCM solution, showing the hydrodynamic diameter of 3.08 ± 1.1 nm. The polydispersity index (PDI) is 0.18.

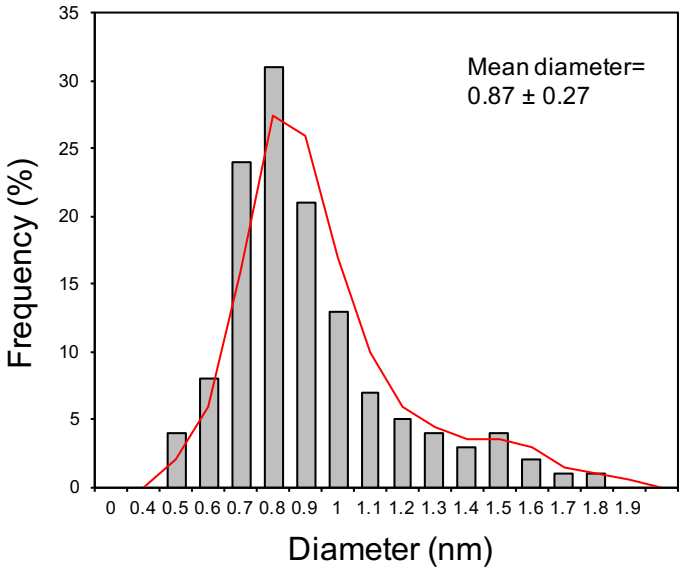

Fig. S4 Particle size distribution histogram acquired from HRTEM image analysis of Au(en)QC samples

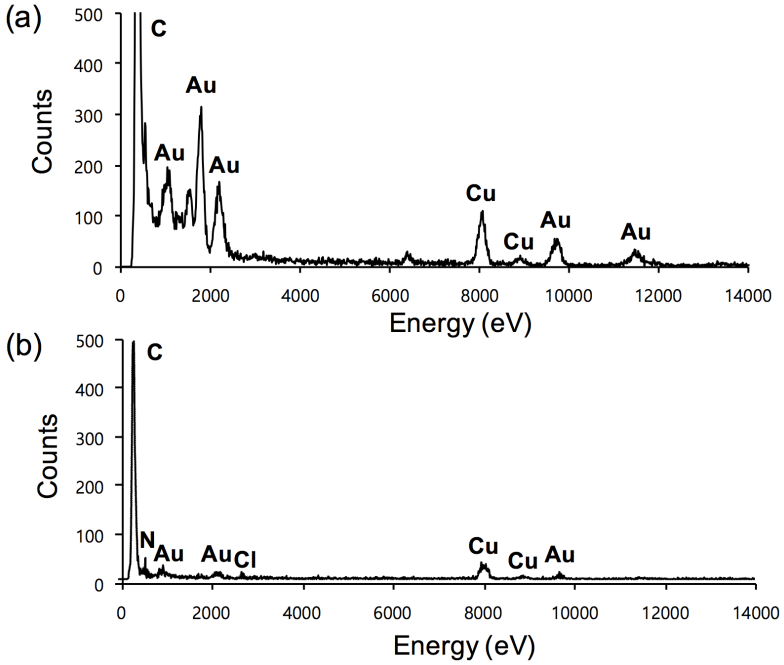

Fig. S5 Energy-dispersive X-ray (EDX) spectra of (a) Butanethiol-AuNPs and (b) Au(en)QCs.

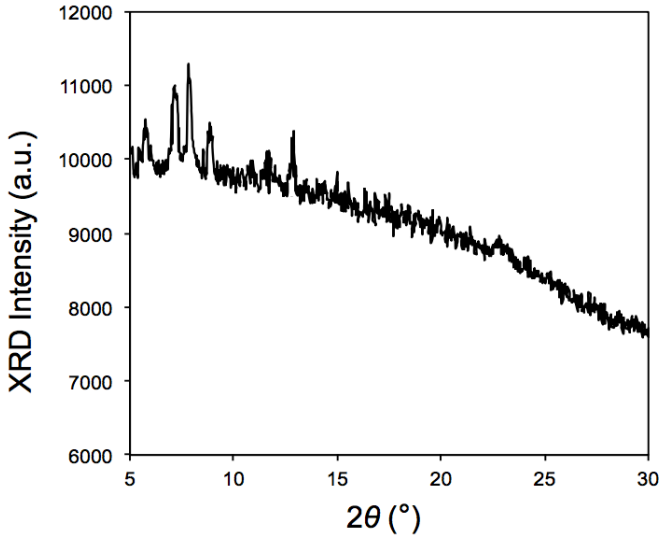

Fig. S6 Powder XRD pattern of Au(en)QC sample

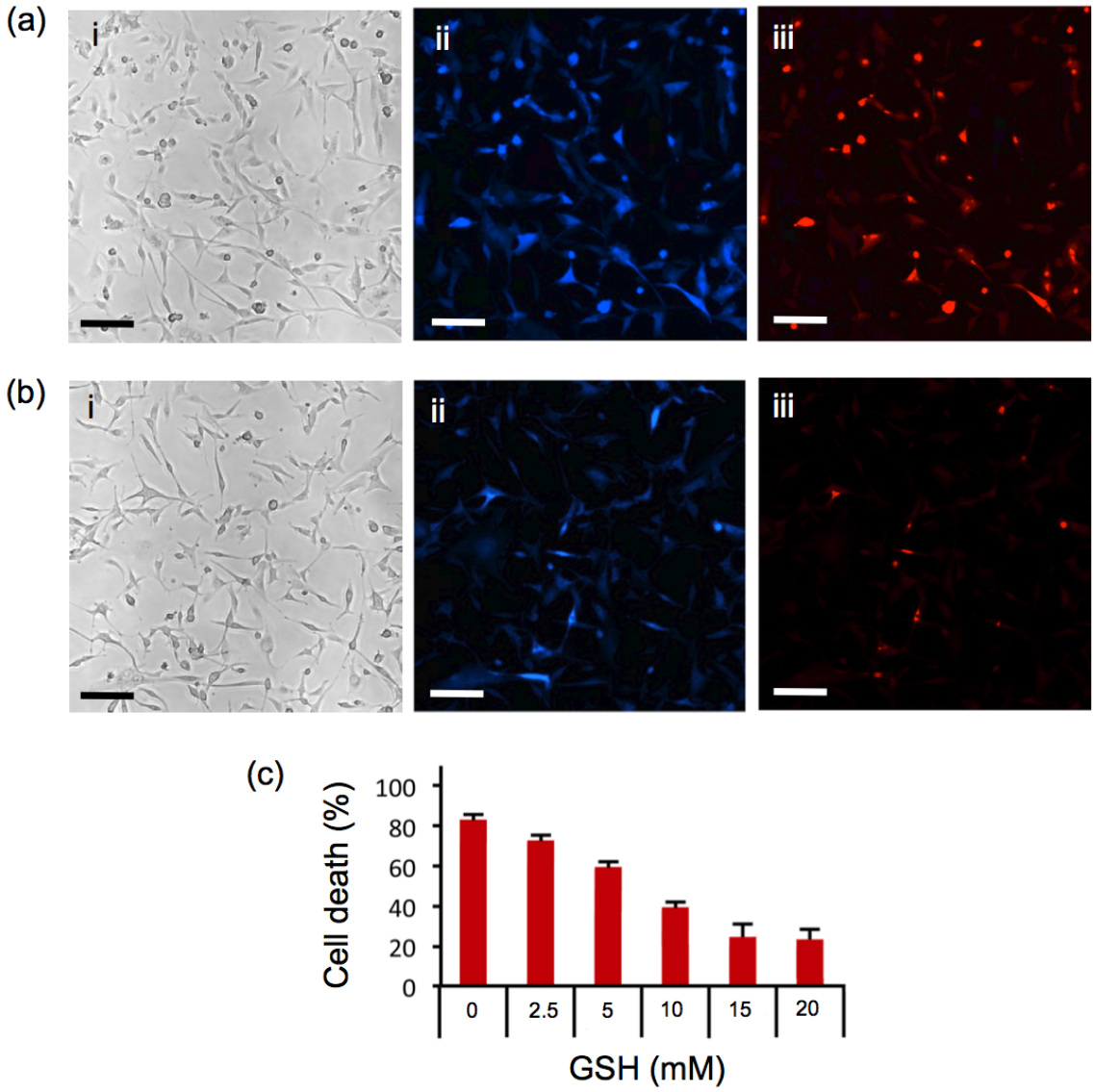

Fig. S7 Effect of GSH on cytotoxicity of Au(en)QCs. Confocal microscopic images of A2780 cells after incubation with 20 μM Au(en)QCs for 24 h, in the (a) absence/ (b) presence of 20 mM GSH. (i) Bright field, (ii) DAPI, and (iii) PI modes were shown. (c) XTT assay. Scale bar: 200 μm.

1

2

(a)

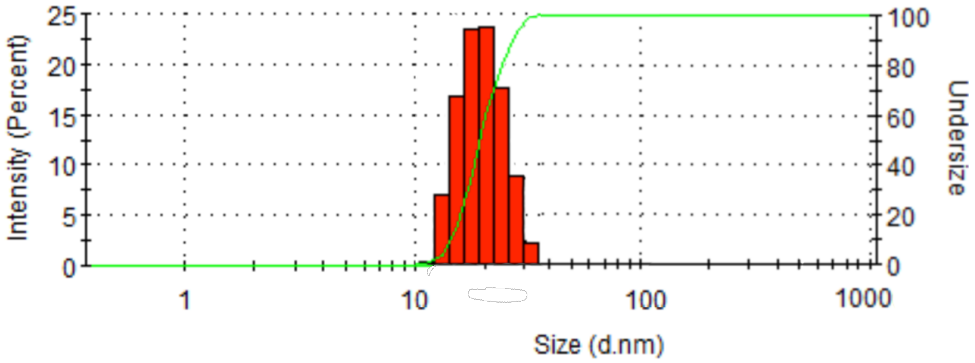

(b)

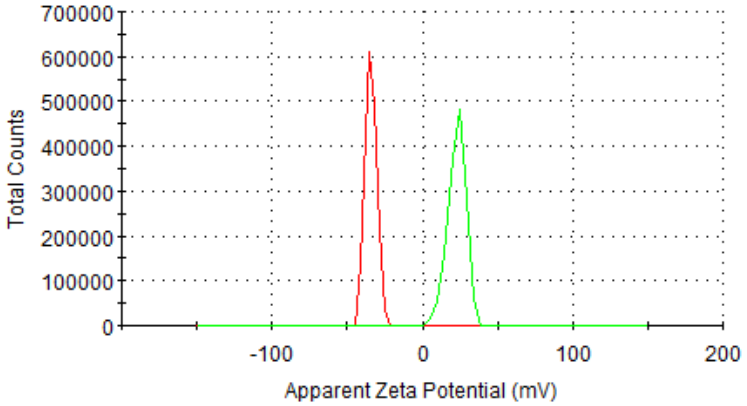

3

4 **Fig. S8** (a) DLS size distribution of Tf-Au(en)QC solution (the polydispersity

5 index (PDI) is 0.24) and (b) the colloidal stability determination of Au(en)QCs (green

6 peak) and Tf-Au(en)QCs (red peak) by zeta potential analysis.

7

8

9

10

11

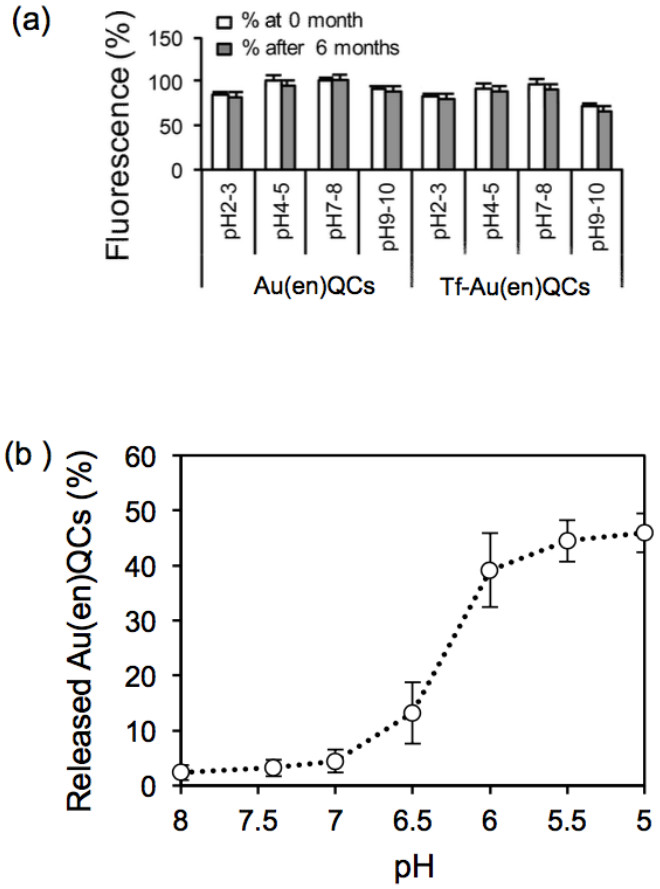

Fig. S9 (a) pH-dependent photostability of Au(en)QCs and Tf-Au(en)QCs before and after 6 months. (b) pH-dependent release profile of Au(en)QCs from Tf-Au(en)QCs.

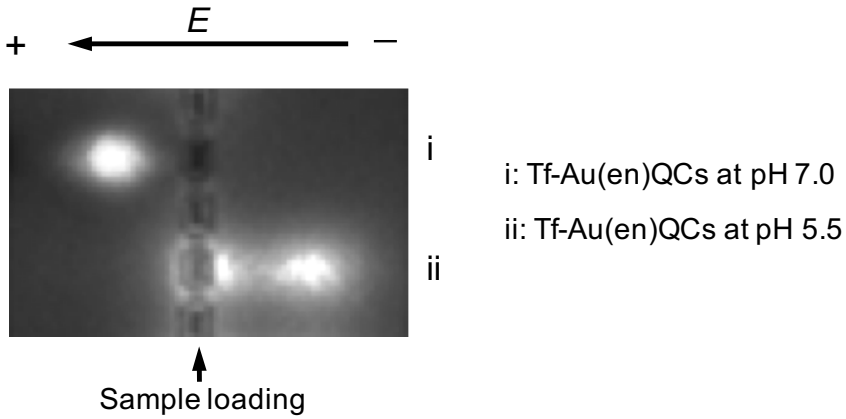

Fig. S10 Gel electrophoretic analysis of the Tf-Au(en)QC samples at different biological pH, which displayed the dissociation of Au(en)QCs from the Tf-Au(en)QC complexes at pH 5.5

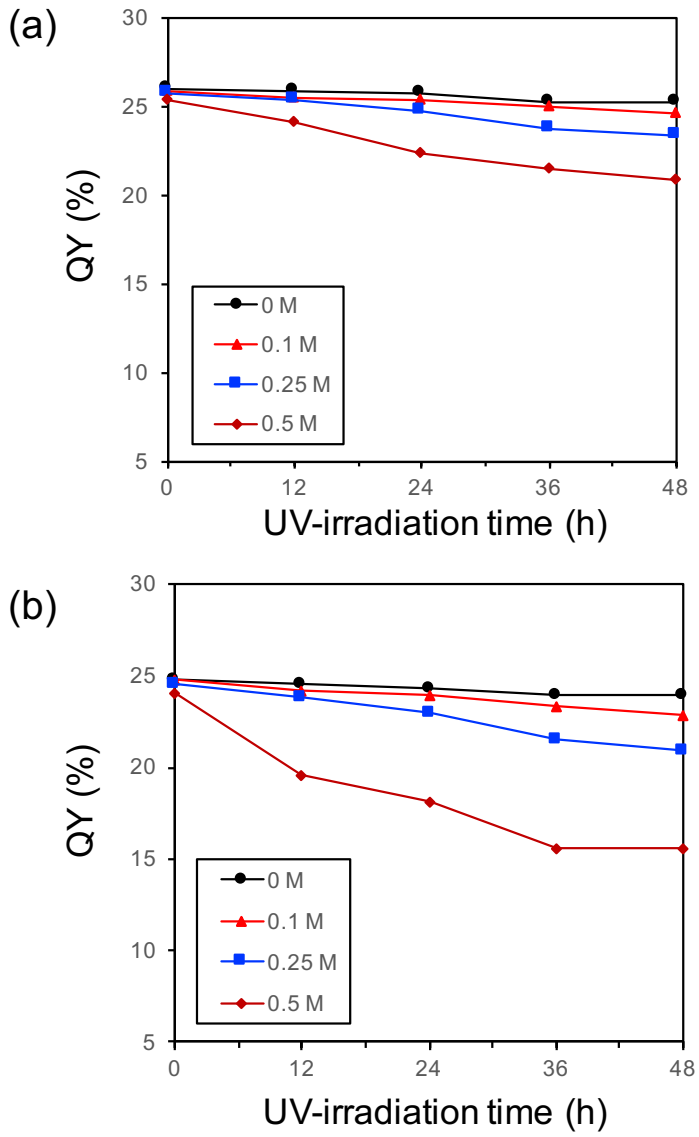

Fig. S11 Effect of salt and photoirradiation on colloidal stability of (a) AuQCs and (b) Tf-AuQCs for 2 days. The QY levels were measured by PL-spectroscopy at $\lambda_{em,\ max}$=473 nm in the absence/presence of NaCl, as a function of time under an UV-lamp (365 nm).

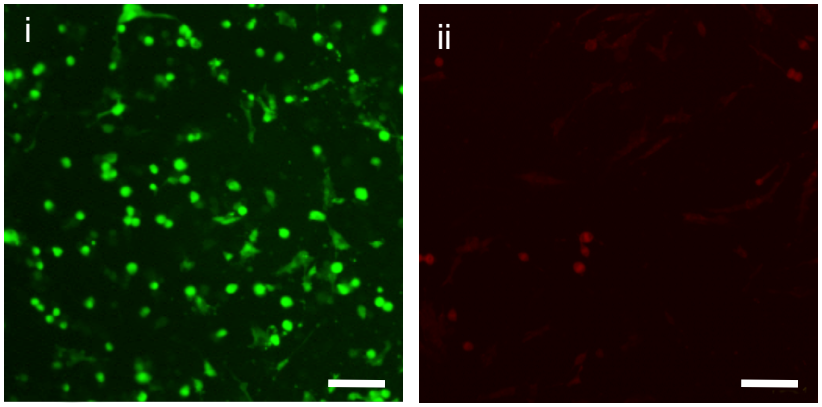

Fig. S12 Live/dead cancer cell imaging to examine effect of an excessive apo-Tf proteins (40 μM) as a control experiment: The cells were treated only with free apo-Tf proteins without adding Tf-Au(en)QCs. Microscopic images of viable ovarian carcinoma cells (A2780) stained with calcein AM (i) and PI (ii), showing no evident dead cells. Scale: 200 μm.

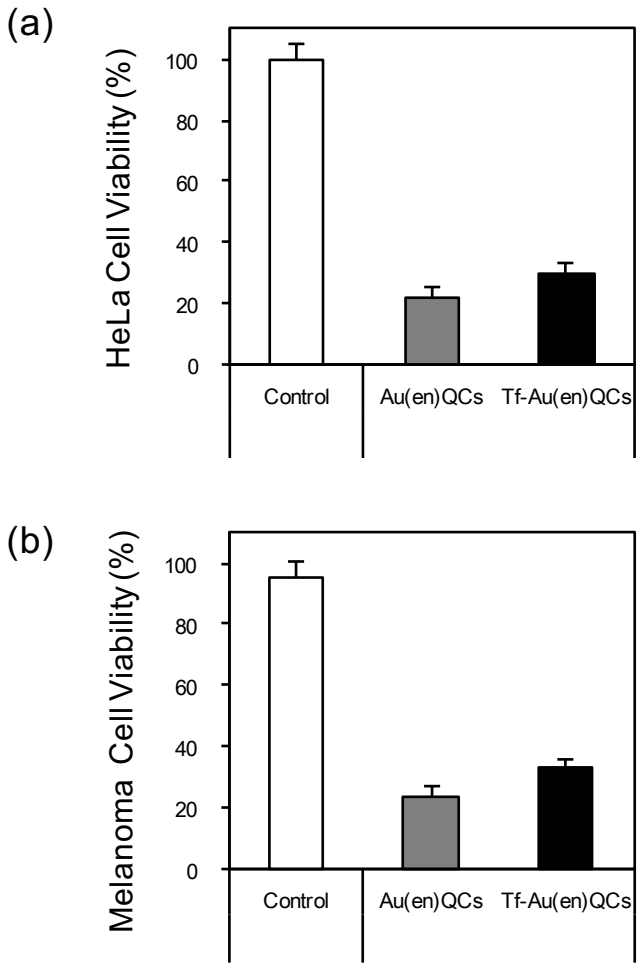

Fig. S13 XTT assays of Au(en)QC and Tf-Au(en)QC samples over (a) HeLa and (b) human melanoma cancer cells.